Isotopic Disequilibrium during Uptake of Atmospheric CO_2 into Mine Process Waters: Implications for CO_2 Sequestration

SIOBHAN A. WILSON,*,† SHAUN L. L. BARKER,† GREGORY M. DIPPLE,†,‡ AND VIOREL ATUDOREI§

Mineral Deposit Research Unit, Department of Earth and Ocean Sciences, The University of British Columbia, 6339 Stores Road, Vancouver, British Columbia V6T 1Z4, Canada, Pacific Centre for Isotopic and Geochemical Research, Department of Earth and Ocean Sciences, The University of British Columbia, 6339 Stores Road, Vancouver, British Columbia V6T 1Z4, Canada, and Department of Earth and Planetary Sciences, The University of New Mexico, MSCO3-2040, 1 University of New Mexico, Albuquerque, New Mexico 87131-0001, United States

Received June 22, 2010. Revised manuscript received October 12, 2010. Accepted November 4, 2010.

Dypingite, a hydrated Mg-carbonate mineral, was precipitated from high-pH, high salinity solutions to investigate controls on carbon fixation and to identify the isotopic characteristics of mineral sequestration in mine tailings. $\delta^{13}C$ values of dissolved inorganic carbon content and synthetic dypingite are significantly more negative than those predicted for equilibrium exchange of CO_2 gas between the atmosphere and solution. The measured $\delta^{13}C$ of aqueous carbonate species is consistent with a kinetic fractionation that results from a slow diffusion of atmospheric CO_2 into solution. During dypingite precipitation, dissolved inorganic carbon concentrations decrease and $\delta^{13}C$ values become more negative, indicating that the rate of CO_2 uptake into solution was outpaced by the rate of carbon fixation within the precipitate. This implies that CO_2 gas uptake is rate-limiting to CO_2 fixation. $\delta^{13}C$ of carbonate mineral precipitates in mine tailings and of DIC in mine process waters display similar ^{13}C-depletions that are inconsistent with equilibrium fractionation. Thus, the rate of carbon fixation in mine tailings may also be limited by supply of CO_2. Carbon sequestration could be accelerated by increasing the partial pressure of CO_2 in tailings ponds or by using chemicals that enhance the uptake of gaseous CO_2 into aqueous solution.

Introduction

Secondary hydrated Mg-carbonate minerals that form within ultramafic tailings from some mines are safe and durable traps for carbon (*1*). Mineralization of carbon dioxide (CO_2) in ultramafic mine tailings can occur on a scale that is significant relative to the greenhouse gas emissions of mine operations, and it has been suggested that carbonation of Mg-silicate mine tailings may be used by some mining operations to offset their greenhouse gas emissions (*2*). Furthermore, if carbon fixation could be accelerated, the capacity for carbon fixation in large individual mines is millions of tons of CO_2 per year (*2*).

Several carbon reservoirs can be tapped during carbon fixation within mine tailings (*2*). In order to establish that atmospheric CO_2 is being fixed, it is necessary to fingerprint the carbon found within secondary carbonate minerals. One way of fingerprinting the source of carbon is through the use of stable carbon isotopes (e.g., $\delta^{13}C$). While useful in many fields of the Earth sciences, the interpretation of the stable isotopic compositions of hydrated Mg-carbonate minerals is hampered by an incomplete knowledge of isotopic fractionation between CO_2 gas, dissolved inorganic carbon (DIC), and minerals. Radiocarbon isotopic data confirm that the tailings of several mines are sequestering CO_2 from the modern atmosphere (*2, 3*). Thus, stable carbon isotopic data may be most useful to infer processes by which carbon is transferred within mine tailings environments, rather than to fingerprint the source of carbon, in a similar way to which oxygen isotopes may be used to track processes that cycle oxygen.

Here, we present mineralogical and stable isotopic data from Mg-carbonate precipitation experiments designed to mimic mine process waters. Laboratory air, including atmospheric CO_2, is bubbled through high-pH, high salinity solutions in order to assess how carbon isotopes are fractionated during fixation in mineral form. These data are used to identify important controls on carbon fixation rates and to provide information on carbon isotopic fractionation between CO_2 gas, dissolved inorganic carbon (DIC), and minerals.

Methods

Two identical benchtop precipitation experiments (called experiments 1 and 2) were run simultaneously under ambient conditions. Both experiments initially contained 1.00 mol/L NaCl (Fisher Scientific, Certified ACS Sodium Chloride), 0.100 mol/L $MgCl_2$ (Sigma-Aldrich, Anhydrous Magnesium Chloride assayed at ≥98% purity), and 2.5×10^{-2} mol/L NaOH (Fisher Scientific, Certified ACS Sodium Hydroxide). The pH of each experiment was allowed to drift as the solution evaporated and the precipitation reaction progressed. Carbon was introduced into the experiments by bubbling laboratory air into solution using a peristaltic pump. A small sample of precipitate was collected daily from each experiment for measurement of $\delta^{13}C$ and $\delta^{18}O$ values and phase identification with X-ray powder diffraction (XRPD). Daily measurements were taken of pH, temperature, and total mass of the experiments before and after sampling. For simplicity, precipitate phases are referred to by their mineral names in this paper. Samples of water for measurement of total dissolved inorganic carbon (DIC), $\delta^{18}O$ of water, and $\delta^{13}C$ of DIC were also collected. Detailed experimental methods are provided in the Supporting Information (SI).

Analytical Results

1. Data from Monitoring of Temperature, pH, and Mass Loss. Daily measurements of temperature, pH, and mass loss due to evaporation and sampling are summarized in SI Tables S2 and S3 and Figure 1. Solution temperatures were

* Corresponding author phone: (812)675-4939; fax: (812)855-7899; e-mail: siowilso@indiana.edu. Current address: Department of Geological Sciences, Indiana University, 1001 East 10th Street, Bloomington, IN 47405-1405, USA.
† Mineral Deposit Research Unit, Department of Earth and Ocean Sciences, The University of British Columbia.
‡ Pacific Centre for Isotopic and Geochemical Research, Department of Earth and Ocean Sciences, The University of British Columbia.
§ Department of Earth and Planetary Sciences, The University of New Mexico.

10.1021/es1021125

Published on Web 11/17/2010

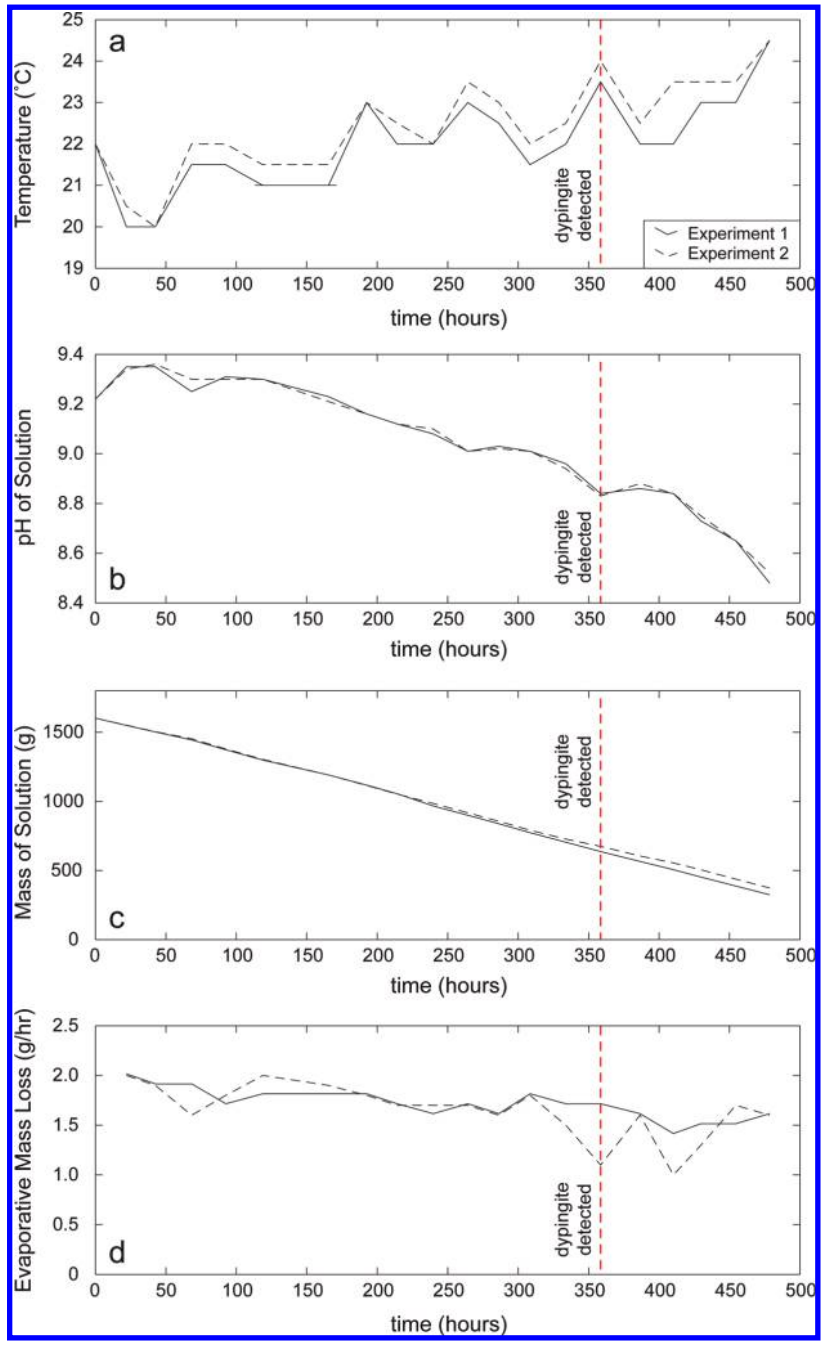

FIGURE 1. Temperature (°C), pH, and water loss from solutions over time. Variation of temperature with time is plotted in (a), variation of pH with time is plotted in (b), mass of solution over time is plotted in (c), and (d) gives average hourly mass loss from solutions between measurements. The time corresponding to collection of samples in which dypingite was first detected is marked by a dashed line.

allowed to drift freely under ambient conditions. Temperatures varied between 20.0° ± 0.5 °C and 24.5° ± 0.5 °C, and a general trend toward increasing temperature was observed with time (Figure 1a).

Both experimental solutions began with a pH of 9.22. The pH declined slowly to a value of approximately 8.9 when dypingite precipitated on the sixteenth day of the experiments (Figure 1b). At this point pH began to change more rapidly, reaching a final value of approximately 8.5 in both experiments.

Mass was lost due to evaporation and sampling of solution and precipitates (Figure 1c). Mass loss by evaporation is typically about twice that of the mass lost to sampling. Between 1.4−2.0 g/hour of water were lost to evaporation from experiment 1 and 1.0−2.0 g/hour of water were lost from experiment 2 (Figure 1d).

2. Results of Total Dissolved Inorganic Carbon Measurements. The concentration of total dissolved inorganic carbon (DIC) was measured for 10 samples from each experiment (SI Tables S2 and S3 and Figure 2a). Measurements of DIC concentrations were made on samples of water collected on alternating days so that the remaining samples could be analyzed for stable isotopic compositions. Initially low DIC concentrations increased by an order of magnitude, reaching their highest measured values (151.7 mg/L and 135.4 mg/L for experiments 1 and 2, respectively) at the onset of carbonate precipitation. Once carbonate precipitates had begun to form, DIC concentrations declined until the experiments were concluded.

3. Characterization of Precipitates. Synthetic mineral identifications from X-ray powder diffraction patterns are

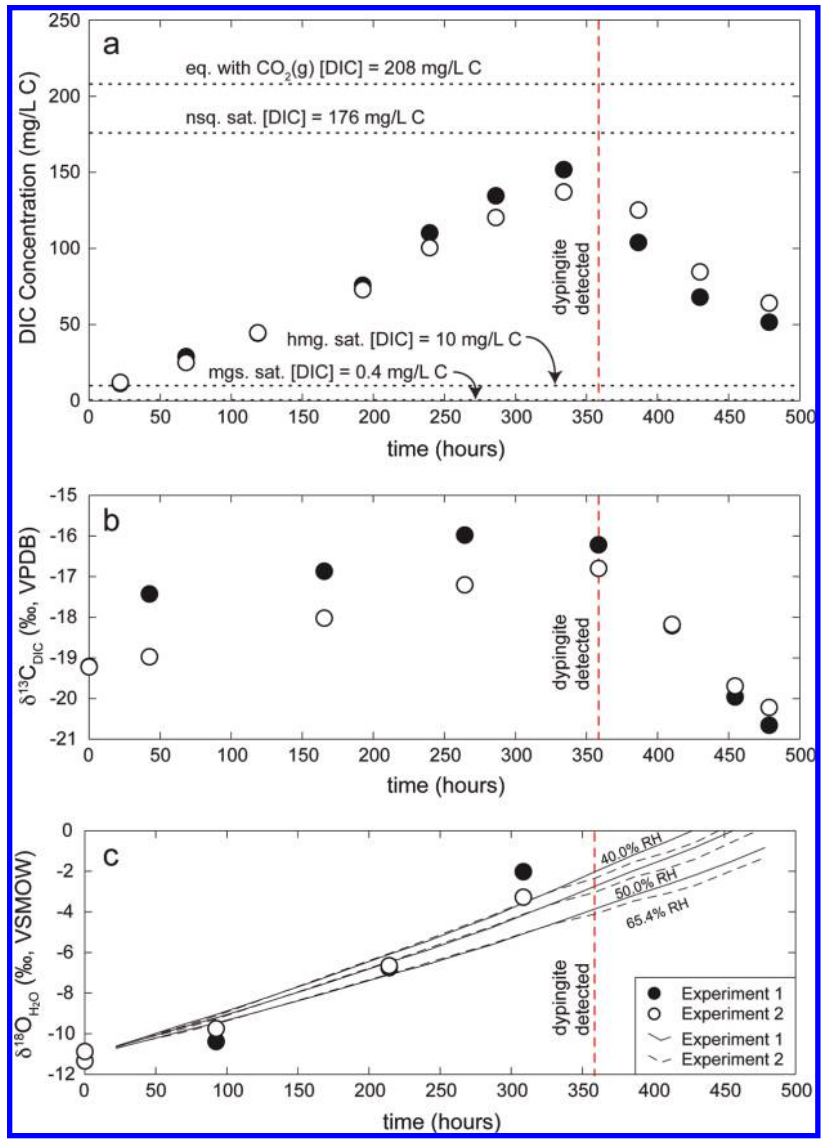

FIGURE 2. Stable carbon and oxygen isotopic data and concentrations of dissolved inorganic carbon (DIC) over time. Concentrations of DIC in solution are given with PHREEQC model results in (a), δ^{13}C (VPDB) values of DIC are given in (b), and δ^{18}O (VSMOW) values of water are shown in (c). Evaporative water loss is modeled as a Rayleigh distillation effect in (c) at three different values of relative humidity. Uncertainties on measured values are smaller than the symbols employed. The time corresponding to collection of samples in which dypingite was first detected is marked by a dashed line.

summarized in the last three columns of SI Tables S2 and S3. XRPD patterns and elemental abundance data are given in SI Figure S1 and SI Table S4, respectively.

Precipitates were not obtained in sufficient quantity for collection of XRPD patterns from either experiment on days 1−3, from experiment 1 on day 13, and from experiment 2 on day 10. No sampling was done on day 7. From the fourth day until the sixteenth day of both experiments, poorly crystalline brucite (characterized by broad, asymmetric peaks) was the most abundant crystalline phase in the precipitates and was accompanied by a lesser amount of halite that had precipitated along the interior walls of the beakers and as a crust on the tubing. Synthetic dypingite [$Mg_5(CO_3)_4(OH)_2 \cdot \sim 5H_2O$] was first identified in both experiments on day 16. By the seventeenth day, dypingite was the most abundant phase, and the relative amount of brucite had declined.

In experiment 1, the amount of brucite continued to decline. On day 19 of this experiment, brucite was observed only at trace abundance, and by day 20 it was no longer detectable. Contrastingly, a small proportion of brucite remained detectable in precipitates from experiment 2 up to and including day 21 of the experiment (see the SI).

4. Stable Isotopic Results. The stable carbon isotopic composition of total dissolved inorganic carbon (DIC) was measured for eight samples of filtered water from each experiment (SI Tables S2 and S3 and Figures 2b and 3). At the onset of experiments 1 and 2, $\delta^{13}C_{DIC}$ values were −19.2‰ and −19.3‰ (VPDB), respectively. $\delta^{13}C_{DIC}$ values became progressively more positive over time, reaching maximum measured values on day 16 (exp. 2) or just before (exp. 1) the onset of dypingite precipitation. Maximum values of $\delta^{13}C_{DIC}$ were −16.0‰ and −16.9‰ (VPDB) for experiments 1 and 2, respectively. After day 16, once dypingite had begun to form, $\delta^{13}C_{DIC}$ values became progressively more negative.

Stable oxygen isotopic compositions were determined for eight samples of filtered water. Results for three samples from each experiment and two identical samples of the Nanopure water used to prepare experimental solutions are listed in SI Tables S2 and S3 and plotted in Figures 2c and 3. Analyses of the duplicate samples of Nanopure water give $\delta^{18}O_{H2O(l)}$ values of −11.3‰ and −10.9‰ (VSMOW). Water

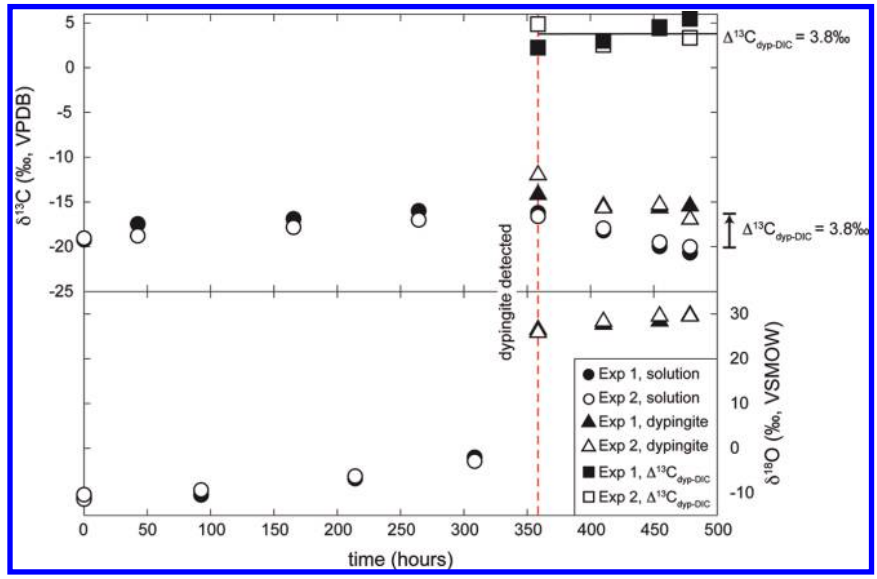

FIGURE 3. Stable carbon and oxygen isotopic data for synthetic dypingite, dissolved inorganic carbon (DIC), and water. $\delta^{13}C$ values are given relative to VPDB, and $\delta^{18}O$ values are given relative to VSMOW. Uncertainties on measured values are smaller than the symbols employed. The time corresponding to collection of samples in which dypingite was first detected is marked by a dashed line.

sampled from the experiments becomes progressively more enriched in ^{18}O with time. On day 14, the last day for which there are $\delta^{18}O_{H2O(l)}$ data, water from experiment 1 has a value of $\delta^{18}O_{H2O(l)} = -2.0‰$ (VSMOW) and water from experiment 2 gives $\delta^{18}O_{H2O(l)} = -3.4‰$ (VSMOW).

Stable oxygen and carbon isotopic data were obtained for four specimens of dypingite from each experiment. Precipitates of dypingite from days 16, 18, 20, and 21 were analyzed from both experiments (SI Tables S2 and S3 and Figure 3). Dypingite from experiment 1 gives $-15.4‰ \leq \delta^{13}C_{dyp} \leq -14.0‰$ (VPDB) and $27.0‰ \leq \delta^{18}O_{dyp} \leq 30.2‰$ (VSMOW). Experiment 2 yielded dypingite with a broader range of values: $-16.9‰ \leq \delta^{13}C_{dyp} \leq -12.0‰$ (VPDB) and $25.8‰ \leq \delta^{18}O_{dyp} \leq 29.5‰$ (VSMOW).

Discussion

1. Mineralogy of Final Precipitates. Both experiments precipitated dypingite [$Mg_5(CO_3)_4(OH)_2 \cdot \sim 5H_2O$] at the expense of brucite [$Mg(OH)_2$]. Brucite is known to weather to hydromagnesite [$Mg_5(CO_3)_4(OH)_2 \cdot 4H_2O$] under conditions of temperature and pressure that prevail at the Earth's surface (*4*). In addition, Botha and Strydom (*5*) and Xiong and Lord (*6*) have synthesized hydromagnesite by slow replacement of brucite in aqueous solution. Zhao et al. (*7*) have also produced minor amounts of hydromagnesite and dypingite as accessory phases to nesquehonite [$MgCO_3 \cdot 3H_2O$] produced by rapid replacement of brucite. The gradual decline in the relative abundance of brucite (and its complete consumption in exp. 1) suggests that dypingite, like hydromagnesite and nesquehonite, can form by the carbonation of brucite. Brucite is a common gangue mineral in the tailings of some mining operations and mineral abundance data show that brucite dissolution accompanies Mg-carbonate mineral precipitation in mine tailings at the Mount Keith Nickel Mine in Western Australia (*8*).

2. Isotopic Composition of Laboratory Atmosphere and Solution. In the range of pH under which experiments were conducted (i.e., 8.48−9.36) bicarbonate is known to be the dominant aqueous carbonate species by several orders of magnitude (*9*). The value for the $\delta^{13}C$ of CO_2 in our laboratory's atmosphere was measured to be $-8 \pm 1‰$ (VPDB) shortly after precipitation experiments were conducted (measured using a Carbon Dioxide Isotope Analyzer from Los Gatos Research, Inc.). Using the measured $\delta^{13}C$ value of laboratory CO_2 and the equilibrium carbon isotopic fractionation factor of Mook et al. (*10*), $10^3 \ln\alpha_{HCO3^- - CO2(g)} = 7.9‰$ at 25 °C, DIC in equilibrium with the laboratory atmosphere should be characterized by $\delta^{13}C_{DIC} \approx 0‰$ (VPDB). The $\delta^{13}C_{DIC}$ of the experiments is highly depleted relative to this expected equilibrium value, which could be explained by (1) kinetic fractionation of carbon isotopes during uptake of CO_2 gas into solution or (2) an unmeasured excursion of extremely ^{13}C-depleted CO_2 gas.

A potential cause of the depleted $\delta^{13}C$ signature of DIC in the precipitation experiments is a kinetic fractionation effect that can accompany diffusion of gaseous CO_2 into a solution. O'Neil and Barnes (*11*) and Clark et al. (*12*) describe near-instantaneous precipitation of travertines and "scums" made of calcite and aragonite from high-pH (i.e., pH > 11), $Ca^{2+}-OH^-$-waters. O'Neil and Barnes (*11*) observed extreme depletion of ^{13}C in the resulting calcite and aragonite and explained this depletion using Graham's Law, $\alpha_{m^*-m} = (m/m^*)^{1/2}$, in which α is the observed diffusive fractionation between a molecule of mass m^* that bears a heavier isotope and a molecule of mass m that bears a lighter isotope. Considering the diffusion of $^{13}CO_2$ relative to $^{12}CO_2$, and assuming that these molecules can be modeled as point masses exhibiting simple harmonic motion, O'Neil and Barnes (*11*) predicted that a kinetic isotope effect of ∼−11.2‰ would accompany diffusion of gaseous CO_2 into high-pH, $Ca^{2+}-OH^-$-water. Using the measured $\delta^{13}C$ value for laboratory CO_2 gas of -8 ± 1 ‰ (VPDB), the kinetic diffusion effect proposed by O'Neil and Barnes (*11*) would produce aqueous bicarbonate with $\delta^{13}C_{DIC} \approx -20‰$ to $-18‰$ (VPDB), which is consistent with the initial carbon isotopic composition of DIC in both experiments (i.e., −19.3‰ to −19.2‰, VPDB). Because our experimental results are consistent with this theoretical prediction, we dismiss as highly unlikely the possibility that the depleted $\delta^{13}C$ signature of the DIC is the result of an unmeasured excursion of anomalously light CO_2 in our laboratory atmosphere. Clark et al. (*12*) considered diffusion fractionation as a mechanism that could lead to the depletion in ^{13}C they observed in both carbonate travertines in northern Oman and barium carbonate precipitated in laboratory experiments. However, they did not monitor $\delta^{13}C$ of DIC, and their experiments resulted in a kinetic fractionation of a different magnitude than that predicted by Graham's Law and demonstrated in our study.

It can be seen from Figure 2b that $\delta^{13}C_{DIC}$ values become increasingly positive with time. This trend toward enrichment in ^{13}C is consistent with either very slow diffusion of atmospheric CO_2 into solution or degassing of light CO_2 from solution. Comparison of the trends in $\delta^{13}C_{DIC}$ with the concentration of DIC over time (Figure 2a) demonstrates a contemporaneous increase in DIC concentration with ^{13}C-enrichment. Thus, degassing is dismissed as a possibility. The increase in DIC concentrations was driven by slow uptake of atmospheric CO_2 and by evapoconcentration. Evapoconcentration accounts for about 10% of the increase in DIC concentration. Geochemical modeling using PHREEQC (*13*) and the Pitzer database indicates that the equilibrium concentration of DIC for these experiments is 208 mg/L C at atmospheric CO_2 pressure. Modeling replacement of brucite by Mg-carbonate minerals, using the Pitzer and wateq4f databases, indicates that our experimental solutions should become saturated with respect to nesquehonite at a DIC concentration of 176 mg/L C, to hydromagnesite at a concentration of 10 mg/L C, and to magnesite at a concentration of 0.4 mg/L C. No data were available to model precipitation of dypingite. Precipitation of hydromagnesite and magnesite is not kinetically favored at low temperatures, and the model for nesquehonite indicates that the equilibrium DIC concentration must increase to reach saturation of the experimental solutions with respect to this low-temperature Mg-carbonate mineral. However, a significant decrease in DIC concentration and progressively more negative $\delta^{13}C_{DIC}$ values are coincident with the detection of dypingite precipitation on day 16. Thus it appears that DIC concentrations in the experiments did not attain equilibrium with atmospheric CO_2 and that the divergence from equilibrium increased upon precipitation of dypingite.

The fractionation of oxygen isotopes in these experiments can be described by evaporative loss of ^{16}O at moderate humidity. This effect is modeled in Figure 2c as a Rayleigh process using measured values of $H_2O(l)$ loss by evaporation, Δm (from SI Tables S2 and S3), and Gonfiantini's (*14*) relation for the humidity-dependence of kinetic isotopic fractionation of oxygen during evaporation

$$\delta^{18}O_{H2O(l)} = (\varepsilon_{H2O(g)-H2O(l)} + \Delta\varepsilon_{H2O(g)-H2O(l)}) \cdot \ln f + \delta^{18}O_{H2O(l)o} \quad (1)$$

where $\varepsilon_{H2O(g)\text{-}H2O(l)}$ is the equilibrium isotopic separation factor between water vapor and liquid water, f is the fraction of liquid water remaining, and $\delta^{18}O_{H2O(l)o}$ is the initial oxygen isotopic composition of the solution. $\Delta\varepsilon_{H2O(g)\text{-}H2O(l)}$ describes the humidity-dependent effect of kinetic isotopic fractionation: $\Delta\varepsilon_{H2O(g)\text{-}H2O(l)} = -14.2(1\text{-}h)$‰ for $h \equiv$ relative humidity (RH) (*14*). The equilibrium isotopic separation factor was calculated to be −9.4‰ at 25 °C from the results of Kakiuchi and Matsuo (*15*). $\Delta\varepsilon_{H2O(g)\text{-}H2O(l)}$ was determined for three different values of relative humidity: (1) $\Delta\varepsilon_{H2O(g)\text{-}H2O(l)} = -4.9$‰ at 65.4% RH, which is the average for the month of May (when experiments were conducted) in Vancouver, British Columbia, Canada (*16*), (2) $\Delta\varepsilon_{H2O(g)\text{-}H2O(l)} = -7.1$‰ for RH = 50%, and (3) $\Delta\varepsilon_{H2O(g)\text{-}H2O(l)} = -8.5$‰ for RH = 40%. The data for $\delta^{18}O_{H2O(l)}$ are broadly consistent with kinetic fractionation as a result of evaporation at values of relative humidity between 40% and 65.4%. Mismatches are most likely due to variations in the ambient temperature and relative humidity of the laboratory in which precipitation experiments were conducted. This analysis establishes a kinetic control on the oxygen isotopic composition of the experimental solutions. In addition, it demonstrates the utility of oxygen isotopes for identifying processes occurring during mineral precipitation, in this case significant evaporation driving ^{18}O-enrichment during mineral precipitation.

3. Isotopic Composition of Dypingite. The available $\delta^{18}O_{H2O(l)}$ data do not define a fractionation factor for exchange of oxygen between dypingite and water. However, the available data and simple Rayleigh distillation models suggest that it is on the order of $\Delta^{18}O_{dyp\text{-}H2O(l)} \approx 30$‰ (Figure 3). Assuming that the Rayleigh model for $\delta^{18}O_{H2O(l)}$ using values of $\Delta\varepsilon_{H2O(g)\text{-}H2O(l)} = -4.9$‰ at 65.4% RH is a good approximation to the behavior of the experimental solutions, respective oxygen isotopic fractionations of between 30.4‰ and 31.1‰ (exp. 1) and between 30.0‰ and 31.5‰ (exp. 2) are expected. These predictions are consistent with the equilibrium isotopic fractionation factor of $10^3\ln\alpha_{hydromagnesite\text{-}H2O(l)} = 31.2$‰ that was measured by O'Neil and Barnes (*11*) at 25 °C. Thus, equilibrium exchange of oxygen isotopes appears to have been achieved.

$\delta^{13}C$ values of dypingite and $\delta^{13}C$ values of DIC both become more negative over the same time interval (Figure 3). The fractionation factor between dypingite and DIC ($\Delta^{13}C_{dyp\text{-}DIC}$) is variable between 2.2 and 5.5 ‰ and does not display a clear trend with time. This is likely because while $\delta^{13}C_{DIC}$ may have been homogeneous at any point in time, it is unlikely that $\delta^{13}C$ of a small sampling of dypingite would have been homogeneous, due to continuing precipitation as the $\delta^{13}C$ of DIC evolved. Thus, the variable $\Delta^{13}C_{dyp\text{-}DIC}$ most likely reflects an averaging of the composition of dypingite precipitated over several days.

There are no published equilibrium fractionation factors for carbon isotopic exchange between hydrated Mg-carbonate minerals and CO_2 gas or aqueous carbonate species. The average isotopic fractionation between dypingite and DIC in experiment 1 is 3.8 (±1.4, 1σ)‰ and the value for experiment 2 is 3.8 (±1.1, 1σ)‰. Although carbon isotopic equilibrium between DIC and dypingite was only approached from one direction in these nonreversible experiments, the difference in $\delta^{13}C$ values for dypingite and DIC is consistent with equilibrium fractionation factors for other carbonate minerals, such as magnesite ($\Delta^{13}C_{mag\text{-}HCO3^-} = 6.3$‰ *10, 17*) and malachite ($\Delta^{13}C_{mal\text{-}HCO3^-} = 2.4$‰ *10, 18*). These data yield a provisional equilibrium fractionation factor, $\Delta^{13}C_{dyp\text{-}HCO3^-}$, of 3.8‰.

Trends in DIC concentration and $\delta^{13}C$ are inconsistent with buffering of DIC by influx of atmospheric CO_2. This is implied by both the decline in DIC concentration as dypingite precipitated (i.e., DIC was removed from solution via mineral precipitation faster than it could be replenished by CO_2(g) dissolution) and the change in $\delta^{13}C_{DIC}$ with time as dypingite precipitation occurred. Within these solutions, the exchange of gaseous CO_2 between DIC and the atmosphere is sufficiently slow, at least on the time scale of dypingite precipitation, that the DIC-dypingite system appears to behave as though it were largely closed to the atmosphere for isotopic exchange of carbon. Thus, the precipitation rate of dypingite is likely rate-limited by the dissolution of CO_2 gas into solution.

Implications for CO_2 Sequestration

This study demonstrates that during the uptake of atmospheric CO_2 into high salinity, high-pH solutions, neither DIC concentrations nor $\delta^{13}C_{DIC}$ reach predicted equilibrium values. Moreover upon precipitation of dypingite, DIC concentrations decrease and $\delta^{13}C_{DIC}$ values become increasingly negative, indicating that the rate of dypingite precipitation exceeds the rate at which CO_2 gas can dissolve into solution. Thus, CO_2(g) dissolution is rate-limiting for CO_2 sequestration in this chemical environment.

Our data suggest that environments in which the uptake of CO_2 gas is rate-limited could be identified by DIC concentrations below predicted equilibrium values and by anomalously depleted $\delta^{13}C_{DIC}$ (particularly in the absence of

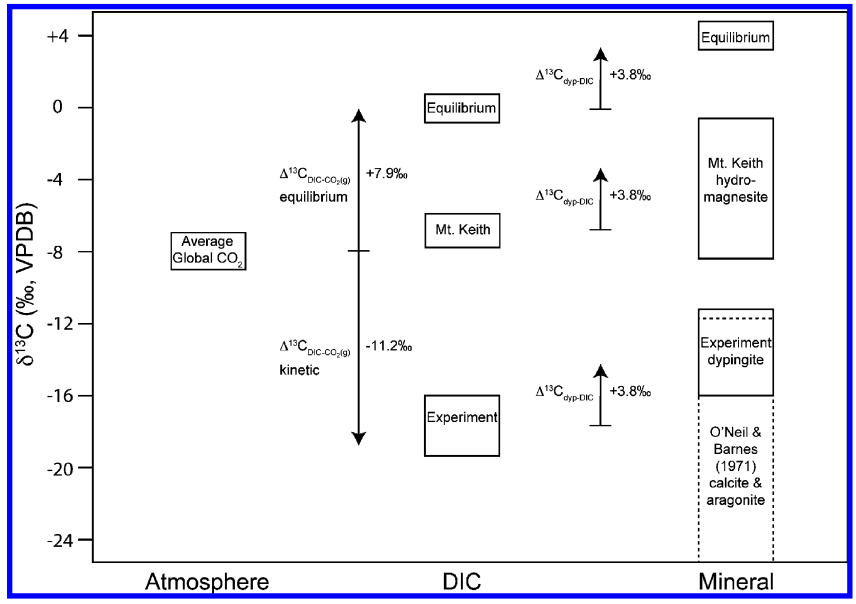

FIGURE 4. Measured $\delta^{13}C$ (VPDB) values of atmospheric CO_2, DIC, experimental precipitates, natural carbonate minerals, and secondary precipitates from mine tailings. Expected equilibrium $\delta^{13}C$ values are calculated using the fractionation factor of Mook et al. (*10*) for exchange of C between aqueous bicarbonate and CO_2(g). Data for naturally occurring carbonate minerals are replotted from O'Neil and Barnes (*11*), and data for secondary hydromagnesite from tailings at the Mount Keith Nickel Mine are replotted from Dipple et al. (*3*).

significant inputs of organic carbon). Environments in which carbonate mineral precipitation is limited by CO_2(g) uptake would produce hydrated Mg-carbonate minerals with significantly depleted $\delta^{13}C$, reflecting equilibrium precipitation from anomalously ^{13}C-depleted DIC.

In high-pH, high salinity environments in California, O'Neil and Barnes (*11*) found that the $\delta^{13}C$ signatures of carbonate minerals associated with serpentinites ranged between −26.1 to −11.0 ‰ (VPDB). O'Neil and Barnes (*11*) describe hydromagnesite, formed by weathering of brucite and serpentine minerals, that was characterized by (1) a depletion in ^{13}C of a similar magnitude to that measured for dypingite in our experiments and (2) $\delta^{18}O$ values consistent with mineral precipitation at oxygen isotopic equilibrium with surface waters (as observed in our experiments). They also reported calcite and aragonite travertines and "scums", precipitated from hyperalkaline waters, which gave significantly more negative $\delta^{13}C$ and $\delta^{18}O$ values than the hydromagnesite (*11*). Clark et al. (*12*) describe calcite travertine deposits from Oman, which give $-28‰ < \delta^{13}C < 0‰$ (VPDB) and $13‰ < \delta^{18}O < 37‰$ (VSMOW) and for which $\delta^{13}C$ and $\delta^{18}O$ data give a linear trend. The experiments of Clark et al. (*11*) show that extremely ^{13}C- and ^{18}O-depleted carbonate minerals form at pH > 11 by (1) kinetic depletion of ^{13}C during hydroxylation of aqueous CO_2 and (2) depletion of ^{18}O via reaction of aqueous CO_2 with OH^- ($\varepsilon^{18}O_{OH^-H2O(l)} \approx -40‰$). Dietzel et al. (*19*) demonstrate convincingly that the rate of CO_2 gas absorption by an alkaline solution is pH-dependent. They suggest that there is a change in the reaction mechanism by which carbonate minerals are precipitated at pH < 11 that is characterized by hydroxylation reactions losing influence over the stable oxygen isotopic signature of carbonate minerals (*19*). Thus, carbonate minerals precipitated from moderately alkaline solutions (pH < 11) are likely to reflect equilibrium values for $\delta^{18}O$.

Several hypotheses have been put forth by previous researchers to explain the less negative, but still depleted, $\delta^{13}C$ values for carbonate minerals precipitated from moderately alkaline solutions (pH < 11) including (1) a mixed organic and atmospheric source of carbon (e.g., refs *2, 19, 20)* or (2) microbial mediation of isotopic signatures (e.g. refs *21*−*23)*. Our experiments suggest that kinetic fractionation of carbon isotopes during diffusion of CO_2(g) into moderately alkaline solutions (in which hydroxylation reactions do not play a significant role in isotopic fractionation) provides a sufficient explanation for modest ^{13}C depletions, at least in environments lacking an abundant source of organic carbon.

Many studies have found that $\delta^{13}C$ and $\delta^{18}O$ data form a positive trend for low-temperature Ca- and Mg-carbonate minerals (e.g., refs *2, 11, 12, 20-25)*. Similar trends have been observed in high-temperature metamorphic environments (*26*) and in pedogenic carbonates precipitated in organic-rich soils (*27*−*29*). Because our experimental data produce a negative trend, in which $\delta^{13}C$ values become more negative as $\delta^{18}O$ values grow more positive, carbon limitation by slow uptake of CO_2 into aqueous solution can be distinguished from the many processes that produce a positive trend in stable carbon and oxygen isotopic data. Nonetheless, our experimental results, when considered with those of Clark et al. (*12*) and Dietzel et al. (*19*), suggest that in some highly alkaline systems the positive, linear relationship between $\delta^{13}C$ and $\delta^{18}O$ data for carbonate minerals may result in part from the pH-dependence of kinetic diffusion fractionation and hydroxylation of CO_2(g) into the solutions from which these minerals formed. This trend may reflect the waning control of hydroxylation reactions at pH < 11 over isotopic fractionation during carbonate precipitation. Because the vast majority of previous laboratory and field-based studies of carbonate mineral precipitation from alkaline solutions have not reported detailed water chemistry, pH, and $\delta^{13}C_{DIC}$ values further experimental study is required to confirm this model.

Our experimental results provide an explanation for variable $\delta^{13}C$ compositions of hydrated Mg-carbonate minerals that does not require involvement of multiple carbon reservoirs. Using ^{14}C as a tracer, Wilson et al. (*2*) found that atmospheric CO_2 was being sequestered into minerals with variable $\delta^{13}C$ signatures, some of which were not consistent with equilibrium precipitation of Mg-carbonate minerals. Ultimately, radiocarbon data proved to be the most reliable mechanism to evaluate trapping of atmospheric carbon within minerals. Wilson et al. (*2*) suggested that the variability in the $\delta^{13}C$ signatures of these minerals could be ascribed to

a mixed atmospheric and organic source of C. The results of this study present the field-based evidence of Wilson et al. (*2*) in a new light and suggest that, in the mine tailings environment, stable isotope data describe the processes by which elements are cycled rather than uniquely revealing their original source. Thus, a more robust tracer, such as radiogenic ^{14}C, should be used for assessing sequestration of atmospheric carbon within mine tailings.

In the ultramafic tailings of the Mount Keith Nickel Mine (Western Australia), the hydrated Mg-carbonate mineral, hydromagnesite, forms as a secondary precipitate (*3*). This hydromagnesite has $\delta^{13}C$ values that range between −8.6 and −1.0 ‰ and average −3.0‰ (VPDB), while process waters ($7 < pH < 9$) have $\delta^{13}C_{DIC}$ between −8.2 and −6.2 ‰ and average −7.4‰ (VPDB). In both natural and engineered environments, like the tailings at Mount Keith, the $\delta^{13}C$ values of carbonate minerals can be significantly more negative than those predicted for minerals precipitating in equilibrium with atmospheric CO_2 (Figure 4). In the case of Mount Keith, where the $\delta^{13}C$ values of both DIC and minerals were measured, the difference in $\delta^{13}C$ is consistent with the equilibrium fractionation factor determined experimentally in this study.

Observed rates of carbon fixation in mine tailings environments, such as that at Mount Keith, are on the order of 50,000 tons of atmospheric CO_2 per year (*3*). Our results suggest that carbon fixation in mine tailings likely occurs in an environment where CO_2(g) uptake into aqueous solution is kinetically inhibited. This implies that the sequestration of CO_2 in mine tailings (*1*−*3*) and in natural ultramafic formations (*30*) could be readily enhanced by either increasing the partial pressure of CO_2 (*7*) or by using chemicals that enhance the uptake of CO_2 gas into aqueous solution (*31*).

Acknowledgments

We acknowledge the support of the Natural Sciences and Engineering Research Council of Canada (NSERC), BHP Billiton, and Diavik Diamond Mines, Inc. through a Collaborative Research and Development Grant to GMD. This project was also supported in part by the Mineralogical Association of Canada through a Student Travel/Research Grant to S.A.W. Work by S.A.W. was supported by a Foundation Scholarship from the Mineralogical Association of Canada and an Alexander Graham Bell Canada Graduate Scholarship from NSERC. We thank Uli Mayer and Anna Harrison for their expertise and help with PHREEQC modeling and James Thom for sharing his knowledge of aqueous geochemistry and for his advice on experimental design. Our thanks go to Shelley Oliver for her generous assistance in minding our experiments. We are grateful to John Kaszuba for his insightful comments on this manuscript, to Peter Kelemen and an anonymous reviewer for careful and perceptive reviews, and to Ruben Kretzschmar for his editorial efforts on our behalf. This is publication 265 of the Mineral Deposit Research Unit.

Supporting Information Available

Detailed description of analytical techniques and mineralogical and geochemical results. This material is available free of charge via the Internet at http://pubs.acs.org.

Literature Cited

(1) Wilson, S. A.; Raudsepp, M.; Dipple, G. M. Verifying and quantifying carbon fixation in minerals from serpentine-rich mine tailings using the Rietveld method with X-ray powder diffraction data. *Am. Mineral.* **2006**, *91*, 1331–1341.

(2) Wilson, S. A.; Dipple, G. M.; Power, I. M.; Thom, J. M.; Anderson, R. G.; Raudsepp, M.; Gabites, J. E.; Southam, G. Carbon dioxide fixation within mine wastes of ultramafic-hosted ore deposits: Examples from the Clinton Creek and Cassiar chrysotile deposits, Canada. *Econ. Geol.* **2009**, *104*, 95–112.

(3) Dipple, G. M.; Wilson, S. A.; Barker, S.; Thom, J. M.; Raudsepp, M.; Power, I.; Southam, G.; Fallon, S. J. Carbon sequestration in ultramafic mine tailings. In *Proceedings of the 10th Biennial Meeting of the SGA, Townsville, Queensland, Australia*; Society for Geology Applied to Mineral Deposits: 2009; pp 762−764.

(4) Hostetler, P. B.; Coleman, R. G.; Mumpton, F. A.; Evans, B. W. Brucite in alpine serpentinites. *Am. Mineral.* **1966**, *51*, 75–98.

(5) Botha, A.; Strydom, C. A. Preparation of a magnesium hydroxy carbonate from magnesium hydroxide. *Hydrometallurgy* **2001**, *62*, 175–183.

(6) Xiong, Y.; Lord, A. S. Experimental investigations of the reaction path in the MgO-CO_2-H_2O system in solutions with various ionic strengths, and their applications to nuclear waste isolation. *Appl. Geochem.* **2008**, *23*, 1634–1659.

(7) Zhao, L.; Sang, L.; Chen, J.; Ji, J.; Teng, H. H. Aqueous carbonation of natural brucite: Relevance to CO_2 sequestration. *Environ. Sci. Technol.* **2010**, *44*, 406–411.

(8) Wilson, S. A. *Mineral traps for greenhouse gases in mine tailings: A protocol for verifying and quantifying CO_2 sequestration in ultramafic mines*. Ph.D. Dissertation, The University of British Columbia, Vancouver, British Columbia, Canada, 2009.

(9) Faure, G. *Principles of Isotope Geology*; Wiley: U.S.A, 1986.

(10) Mook, W. G.; Bommerson, J. C.; Staverman, W. H. Carbon isotope fractionation between dissolved bicarbonate and gaseous carbon dioxide. *Earth Planet. Sci. Lett.* **1974**, *22*, 169–176.

(11) O'Neil, J. R.; Barnes, I. C^{13} and O^{18} compositions in some freshwater carbonates associated with ultramafic rocks and serpentinites: Western United States. *Geochim. Cosmochim. Acta* **1971**, *35*, 687–697.

(12) Clark, I. D.; Fontes, J.-C.; Fritz, P. Stable isotope disequilibria in travertine from high pH waters: Laboratory investigations and field observations from Oman. *Geochim. Cosmochim. Acta* **1992**, *56*, 2041–2050.

(13) Parkhurst, D. L.; Appelo, C. A. J. *User's guide to PHREEQC (version 2) - a computer program for speciation, batch-reaction, one-dimensional transport, and inverse geochemical calculations*; U.S. Geological Survey Water-Resources Investigations Report 99-4259; 1999.

(14) Gonfiantini, R. Environmental isotopes in lake studies. In *Handbook of Environmental Isotope Geochemistry, Vol. 2, The Terrestrial Environment*; Fritz, P., Fontes, J.-C., Eds.; Elsevier: Amsterdam, The Netherlands, 1986; pp 113−168.

(15) Kakiuchi, M.; Matsuo, S. Direct measurements of D/H and $^{18}O/^{16}O$ fractionation factors between vapor and liquid water in the temperature range from 10° to 40°. *Geochem. J.* **1979**, *13*, 307–311.

(16) Environment Canada. National Climate Data and Information Archieve. Vancouver International Airport. Available at http://www.climate.weatheroffice.ec.gc.ca/climate_normals/stnselect_e.html (accessed October 1, 2009).

(17) Zachmann, D. W.; Johannes, W. Cryptocrystalline magnesite. In *Magnesite: Geology, Mineralogy, Geochemsitry, Formation of Mg-Carbonates. Monograph Series on Mineral Deposits*; Möller, P., Ed.; Society for Geology Applied to Mineral Deposits: 1989; Vol. 28, pp 15−28.

(18) Melchiorre, E. B.; Criss, R. E.; Rose, T. P. Oxygen and carbon isotope study of natural and synthetic malachite. *Econ. Geol.* **1999**, *94*, 245–260.

(19) Dietzel, M.; Usdowski, E.; Hoefs, J. Chemical and $^{13}C/^{12}C$- and $^{18}O/^{16}O$-isotope evolution of alkaline drainage waters and the precipitation of calcite. *Appl. Geochem.* **1992**, *7*, 177–184.

(20) Zedef, V.; Russell, M. J.; Fallick, A. E.; Hall, A. J. Genesis of vein stockwork and sedimentary magnesite and hydromagnesite deposits in the ultramafic terranes of southwestern Turkey: A stable isotope study. *Econ. Geol.* **2000**, *95*, 429–446.

(21) Krishnamurthy, R. V.; Schmitt, D.; Atekwana, E. A.; Baskaran, M. Isotopic investigations of carbonate growth on concrete structures. *Appl. Geochem.* **2003**, *18*, 435–444.

(22) Power, I. M.; Wilson, S. A.; Thom, J.; Dipple, G. M.; Southam, G. Biologically induced mineralization of dypingite by cyanobacteria from an alkaline wetland near Atlin, British Columbia, Canada. *Geochem. Trans.* **2007**, *8*, 13.

(23) Power, I. M.; Wilson, S. A.; Thom, J. M.; Dipple, G. M.; Gabites, J. E.; Southam, G. The hydromagnesite playas of Atlin, British Columbia, Canada: A biogeochemical model for CO_2 sequestration. *Chem. Geol.* **2009**, *260*, 286–300.

(24) Kralik, M.; Aharon, P.; Schroll, E.; Zachmann, D. Carbon and oxygen isotope systematics of magnesites. In *Magnesite: Geology, Mineralogy, Geochemsitry, Formation of Mg-Carbonates. Monograph Series on Mineral Deposits*; Möller, P., Ed.; Society for

Geology Applied to Mineral Deposits: 1989, Vol. 28, pp 197−223.
(25) Renforth, P.; Manning, D. A. C.; Lopez-Capel, E. Carbonate precipitation in artificial soils as a sink for atmospheric carbon dioxide. *Appl. Geochem.* **2009**, *24*, 1757–1764.
(26) Baumgartner, L. P.; Valley, J. W. Stable isotope transport and contact metamorphic fluid flow. In *Stable Isotope Geochemistry. Reviews in Mineralogy & Geochemistry*; Valley, J. W., Cole, D. R., Eds.; Mineralogical Society of America and Geochemical Society: 2001, Vol. 43, pp 415−467.
(27) Knauth, L. P.; Brilli, M.; Klonowski, S. Isotope geochemistry of caliche developed on basalt. *Geochim. Cosmochim. Acta* **2003**, *67*, 185–195.
(28) Cerling, T. E. The stable isotopic composition of modern soil carbonate and its relationship to climate. *Earth Planet. Sci. Lett.* **1984**, *71*, 229–240.
(29) Schlesinger, W. H. The formation of caliche in soils of the Mojave Desert, California. *Geochim. Cosmochim. Acta* **1985**, *49*, 57–66.
(30) Kelemen, P. B.; Matter, J. In situ carbonation of peridotite for CO_2 storage. *Proc. Natl. Acad. Sci. U.S.A.* **2008**, *105*, 17295–17300.
(31) Mani, F.; Peruzzini, M.; Stoppioni, P. CO_2 absorption by aqueous NH_3 solutions: Speciation of ammonium carbamate, bicarbonate and carbonate by a ^{13}C NMR study. *Green Chem.* **2006**, *8*, 995–1000.

ES1021125